Measurement of γ rays from antiproton-deuterium annihilation at rest

M. Chiba,[e] T. Fujitani,[d] J. Iwahori,[a,*], M. Kawaguti,[a] M. Kobayashi,[b] S. Kurokawa,[b]
Y. Nagashima,[d] T. Omori,[d,†] S. Sugimoto,[d] M. Takasaki,[b] F. Takeutchi,[c]
Y. Yamaguchi,[d] and H. Yoshida[a,‡]

[a]*Faculty of Engineering, Fukui University, Fukui, Fukui, 910 Japan*
[b]*National Laboratory for High Energy Physics (KEK), Tsukuba, Ibaraki 305, Japan*
[c]*Faculty of Science, Kyoto Sangyo University, Kita, Kyoto, 603 Japan*
[d]*Physics Department, Osaka University, Toyonaka, Osaka, 560 Japan*
[e]*Physics Department, Tokyo Metropolitan University, Hachioji, Tokyo 192-03, Japan*
(Fukui–KEK–Kyoto Sangyo–Osaka–Tokyo Metropolitan Collaboration)

(Received 7 March 1991)

Using modularized NaI(Tl) detectors, we have carried out a high-statistics measurement of inclusive γ-ray spectra from $\bar{p}d$ annihilation at rest separately for each charge multiplicity of the final state. We have not seen, at statistical significance above 4σ, any monochromatic γ-ray peaks, which may be assigned to baryonium production $\bar{p}p$ or $\bar{p}n \to \gamma B$ or to $\bar{N}NN$ bound-state production $\bar{p}d \to \gamma(\bar{N}NN)$. The 4σ upper limit for baryonium production per annihilation varied between 10^{-2} and 10^{-4} depending on baryonium mass of 1700 to 600 MeV/c^2 and on the charge multiplicity. At $(2-3)\sigma$ levels, however, five peaks were observed and three of them are located at the same position with the similar $(2-3)\sigma$ peaks observed in $\bar{p}p \to \gamma B$ and $\bar{p}p \to \pi^0 B$.

I. INTRODUCTION

In previous papers [1,2], we described our experiment searching for narrow γ or π^0 lines from $\bar{p}p$ annihilation at rest in a liquid-H_2 target. The primary physics aim of the experiment was the search for baryonia below the antinucleon-nucleon ($\bar{N}N$) threshold; we denote a proton or a neutron as N throughout the present paper. We obtained a four-standard-deviation (4σ) upper limit of $(1.2-0.2)\times 10^{-3}$ [1] for the yield (i.e., the branching ratio) of $\bar{p}p \to \gamma B$ (here B denotes an antidiquark-diquark baryonium or an $\bar{N}N$ bound state) depending on the γ-ray energy of 80–938 MeV, and a 4σ upper limit of $10^{-2}-10^{-3}$ [2] for $\bar{p}p \to \pi^0 B$ depending on the π^0 energy of 150–900 MeV.

Both Angelopoulos *et al.* [3] and Adiels *et al.* [4] also gave a negative result on baryonia below the threshold at similar sensitivities as in our experiment. Any of the three experiments mentioned above did not confirm the three candidates for baryonia reported before [5] with branching ratios as large as 10^{-3}.

With the same experimental setup as for the $\bar{p}p$ annihilation experiment [1,2], we have also carried out a high-statistics measurement of inclusive γ-ray spectra from $\bar{p}d$ annihilation at rest separately for each charge multiplicity.

The first physics aim of the present measurement is the search for baryonia arising from $\bar{p}n$ annihilation. Should isovector baryonia exist, they may be more clearly observed in the $\bar{p}n$ system than in $\bar{p}p$. In addition to the larger population of the isovector state, another advantage of using the $\bar{p}n$ initial state is that the G-parity conservation in $\bar{p}n \to \gamma B$ is less restrictive than C-parity conservation in $\bar{p}p \to \gamma B$. For example, quantum numbers $J^{PC}=1^{\pm -}$ for B are allowed only from the $^1S_0$ state of $\bar{p}p$ under the S-state dominance hypothesis, while they are allowed from both $^1S_0$ and $^3S_1$ states of $\bar{p}n$. Although B's with $J^{PC}=0^{+-}$, 1^{+-}, 2^{+-} (via $E1$ transition), 1^{-+} ($M1$), etc., are inhibited from $\bar{p}p$, they are allowed from $\bar{p}n$.

Only a few experiments have been reported on narrow ($\bar{p}n$) states below the threshold. A narrow ($\bar{p}n$) state at 1795 MeV/c^2 with the width $\Gamma \leq 8$ MeV/c^2 and $I^G(J^{PC})=1^+(1^{--}, 2^{+-}, 3^{--}$, etc.) was suggested by Gray *et al.* [6] with a branching ratio of the order of 10^{-3} from a measurement of the recoil-proton momentum spectrum in $\bar{p}d \to (\bar{p}n)p$ with a bubble chamber. Amsler *et al.* [7], however, did not confirm the above state from a missing-mass spectrum obtained with a nucleon time-of-flight spectrometer. They gave a 4σ upper limit of 3×10^{-3} for the branching ratio $B(\bar{p}d \to NB)$ in a mass range of $M_B = 1650-1930$ MeV/c^2 for B. They also measured photon spectra searching for narrow states in $\bar{p}d \to NB\gamma$ and obtained a 4σ upper limit of 2×10^{-2}.

Recently, a few candidates of ($\bar{N}N$) quasinuclear states have been suggested ($X(1110)$ with $I^G(J^{PC})=0^+(0^{++})$, $X^0(1480)$ with $0^+(2^{++})$, etc. [8]) from measurement of exclusive channels in $\bar{p}d$ annihilation at rest. Although

their detection in inclusive γ-ray or π^0 spectra should not be straightforward because of their large widths (as large as or larger than several tens of MeV/c^2), there exists an increasing interest in the study of $\bar{p}d$ annihilation at rest.

The second aim is the search for baryonia from $\bar{p}p$ in $\bar{p}d$. The motivation for this search came from the positive signals of narrow γ-ray peaks observed by Adiels *et al.* [9] in $\bar{p}$ ^{4}He annihilation at rest. They observed two narrow peaks in the γ-ray spectrum at 161.9 and 203.0 MeV at statistical significance higher than 4σ, and suggested that baryonia might be produced in nuclei more copiously than in hydrogen.

While $\bar{p}$ annihilation in liquid H_2 is dominated by the initial atomic S state with a small contamination of P state (roughly 20% [10]), $\bar{p}$ annihilation in liquid ^{4}He seems to be dominated by the $(n,L)=2P$ state [11]. Baryonia may become stable by the centrifugal barrier between antinucleon and nucleon in potential models, or between antidiquark and diquark in quarkonium models. Such stabilized baryonia may be more easily produced when the initial orbital angular momentum of the annihilating $\bar{p}$ nucleus is large.

Although there is not yet any clear direct experimental information on the initial atomic state of the annihilating $\bar{p}d$ system, there are some reasons to expect that the amount of P state should be much larger than in $\bar{p}p$ annihilation. This is intuitively understood by comparing $\bar{p}p$ and $\bar{p}d$ atoms with respect to the nuclear radius $R_N(A)=1.3A^{1/3}$ fm and the Bohr radius of $\bar{p}A$ atom given by

$$R_B(\bar{p}A)=n^2\hbar^2/(Z\mu e^2)$$
$$=28.8\ \text{fm}\, n^2(A+1)/(ZA)\ , \qquad (1)$$

where n is the principal quantum number and μ is the reduced mass of $\bar{p}$ and the nucleus A. The Bohr radius for $n=1$ is smaller for $\bar{p}d$ (43.2 fm) than for $\bar{p}p$ (57.6 fm), while the nuclear radius is larger for $\bar{p}d$ (about 4 fm) than for $\bar{p}p$ (about 1.3 fm). Consequently, the overlap of antiproton and nucleus wave functions in the $n=2$ state ($2S$ and $2P$) should be larger in $\bar{p}d$ than in $\bar{p}p$.

Large contribution of $L\geq 1$ $\bar{p}d$ atomic states can also be understood from an intuitive consideration on the orbital angular momentum of antiprotonic atoms. Since the annihilating antiproton will be most dominantly localized at the nuclear surface, it will acquire a kinetic energy in the Coulomb potential, which corresponds to a momentum [9] in the laboratory system of

$$q_{\bar{p}}\sim\hbar(2Z\mu e^2/R_N)^{1/2}$$
$$=51.9[AZ/(A+1)/R_N(\text{in fm})]^{1/2}\ \text{MeV}/c\ . \qquad (2)$$

When annihilation occurs, the impact parameter should be between 0 and $R_N(A)$. Hence, the quantity defined by

$$L_0=q_{\bar{p}}R_N(A) \qquad (3)$$

may give a rough measure for the orbital angular momentum of the annihilating $\bar{p}A$ system. Substituting Eq. (2) into Eq. (3), we get

$$L_0/\hbar=0.263[ZR_N(\text{in fm})A/(A+1)]^{1/2}\ , \qquad (4)$$

which is 0.21, 0.43, and 0.43 for $\bar{p}p$, $\bar{p}d$, and $\bar{p}$ ^{4}He atoms, respectively. Similar magnitudes of L_0 for both $\bar{p}d$ and $\bar{p}$ ^{4}He suggest that $L\geq 1$ initial atomic states may also be important in $\bar{p}d$ annihilation as in $\bar{p}$ ^{4}He [9].

Also, when the $\bar{p}d$ system is taken as an annihilating $\bar{p}p$ plus a neutron, the relatively energetic neutron can carry away a finite angular momentum, thus leaving the $\bar{p}p$ system in a nonzero angular-momentum state.

The above consideration on the orbital angular momentum of annihilating $\bar{p}d$ is supported by the experimental observation of $\bar{p}d$ annihilation at rest into two pions by Gray *et al.* [12] and by Sun *et al.* [13]; both experiments have shown that the orbital angular momentum of $\bar{p}N$ is equal to or larger than 1 for most of the annihilation.

The third aim is the search for $\bar{p}pn$ bound states, which have been predicted in nuclear potential models [14]. Though Dal'karov *et al.* [14] predicted many ($\bar{N}NN$) bound states, narrow ones with a width less than 50 MeV should lie close to the threshold (three times the nucleon mass) with the binding energy less than $\sim$30 MeV. Since our present experiment could measure γ rays above 10 MeV, we could detect some of the bound states if they should exist. The inclusive γ-ray spectra from $\bar{p}d$ annihilation at rest, obtained in the present experiment, is more than an order of magnitude higher in statistics than those [15] reported before.

II. EXPERIMENT AND DATA REDUCTION

The experimental setup was essentially the same as described in [1] except filling liquid D_2 instead of liquid H_2 into the target cell of 14 cm (in diameter)$\times$23 cm (length). Deuterium runs were taken after having completed hydrogen runs.

A secondary antiproton beam at 580 MeV/c from the KEK 12-GeV Proton Synchrotron was made to stop inside the target cell. The emitted γ rays were measured with a modularized NaI(Tl) calorimeter (with 96 modules assembled into a half barrel) covering an effective acceptance of 22% of 4π sr. The charged particles were tracked with cylindrical as well as flat multiwire proportional chambers (MWPC's). Data taking was carried out under a triggering condition of (i) a slow antiproton being incident on the liquid-D_2 cell and (ii) one or two γ rays falling on the NaI.

For 1.92×10^7 triggered events in total, various cuts [1,2] were first applied with respect to hardware errors in readout and in tracking of the degraded antiproton. Requiring then in vertex reconstruction that (i) the vertex should not be located outside the target cell wall by more than 1 cm either radially or longitudinally and that (ii) the rms distance from the vertex to the charged tracks should be less than 1 cm, we obtained 7.32×10^6 events. γ rays were identified by energy deposits in NaI and absence of signal in the scintillator hodoscope and in the MWPC in front of the hit NaI modules. Applying a cluster-finding logic [1], and requiring that the shower leakage into the scintillating glass surrounding the NaI modules should be less than 10% of the γ-ray energy, we finally obtained the total number of γ rays above 10 MeV, N_γ, of 6.70×10^6.

III. ANALYSIS AND RESULT

A. Inclusive γ-ray spectra

The obtained inclusive γ-ray spectra are presented in Fig. 1 for each charge multiplicity, N_{ch}, as well as for the sum over N_{ch}. The number of γ rays in each spectrum is 2.31×10^5 for $N_{ch}=0$, 6.91×10^5 for $N_{ch}=1$, 1.99×10^6 for $N_{ch}=2$, 1.88×10^6 for $N_{ch}=3$, 1.31×10^6 for $N_{ch}=4$, 4.54×10^5 for $N_{ch}=5$, 1.22×10^5 for $N_{ch}=6$, and 2.67×10^4 for $N_{ch}\geq7$.

Table I gives the number of events registered in the γ-ray spectra for each charge multiplicity. The ratio of $\bar{p}p$ to $\bar{p}n$ annihilations, $\alpha/(1-\alpha)$, has been measured in bubble-chamber experiments. Taking an average of four experimental data of 1.31 ± 0.03 [16], 1.33 ± 0.07 [17] and 1.45 ± 0.07 [18], 1.34 ± 0.03 [19], we obtain

$$\alpha/(1-\alpha)=1.33\pm0.02\ ,\qquad \alpha=0.571\pm0.004\ . \tag{5}$$

Since, as shown later, the detection efficiency should be approximately the same both for $\bar{p}p$ and $\bar{p}n$ events, the present $\bar{p}d$ events should consist of 4.18×10^6 $\bar{p}p$ and 3.14×10^6 $\bar{p}n$ annihilations. Using the charge-multiplicity distribution of $\bar{p}p$ events obtained in our experiment [2] with a liquid-H_2 target, we can subtract $\bar{p}p$ from $\bar{p}d$ to deduce the amount of $\bar{p}n$ events for each charge multiplicity; the result is also given in Table I. Events with even charge multiplicities in $\bar{p}n$ annihilation may arise from (i) inefficiency in track reconstruction (about 10% per track) and (ii) conversion of γ rays into e^+e^- pairs (about 6% per γ ray) in and close to the target cell.

B. Narrow peaks in γ-ray spectra

Each γ-ray spectrum, presented in Fig. 1, was fitted with a polynomial background plus narrow Gaussian peaks by using the program MINUIT [20] in a similar way as in [1]. In order to reduce the fitting parameters, we have divided the whole energy range (30–980 MeV) into four with ample overlap between adjacent regions. The order of the polynomial between 2 and 4, mostly 3, was sufficient to give good fits.

In order to search for peaks with the intrinsic width much narrower than the instrumental one, the width of the peaks was restricted to be within $+0\%$, -30% above the instrumental one which was corrected for smearing of γ energy due to the Fermi motion, etc. The asymmetric limits of $+0\%$, -30% were chosen since the instrumental resolution [1] (before correction) was, for safety, overestimated rather than underestimated. The corrected instrumental width [in the full width at half maximum (FWHM)] for the γ energy E can be written as

$$\Delta E/E=[(\Delta E/E)_i^2+(\Delta E/E)_D^2+(\Delta E/E)_S^2]^{0.5}\ \text{(in FWHM)}\ .$$
$$(\Delta E/E)_i=6.2\%/(E\ \text{in GeV})^{1/4}\ ,$$
$$(\Delta E/E)_D=2.36q_{\bar{p}N}/(2\sqrt{3}M_N)\sim0.0478\ , \tag{6}$$
$$(\Delta E/E)_S\sim3q_F^2/(4M_NE)\sim8.6\ \text{MeV}/E\ ,$$

TABLE I. Number of $\bar{p}d$ annihilation events registered in the γ-ray spectra of Fig. 1 is given for each charge multiplicity N_{ch}. It is also divided into $\bar{p}p$ and $\bar{p}n$ annihilation by assuming $\bar{p}d$ annihilation as the sum of quasifree reactions of $\bar{p}p$ and $\bar{p}n$ annihilations (see the text).

N_{ch}	$\bar{p}d$ (measured)	$\bar{p}p$ (deduced)	$\bar{p}n$ (deduced)
0	1.96×10^5	1.71×10^5 (4.1%)	2.43×10^4 (0.8%)
1	6.04×10^5	2.51×10^5 (6.0%)	3.54×10^5 (11.3%)
2	1.94×10^6	1.33×10^6 (31.9%)	6.07×10^5 (19.3%)
3	2.07×10^6	9.10×10^5 (21.8%)	1.16×10^6 (36.9%)
4	1.63×10^6	1.08×10^6 (25.8%)	5.55×10^5 (17.7%)
5	6.39×10^5	3.01×10^5 (7.2%)	3.39×10^5 (10.8%)
6	1.90×10^5	1.09×10^5 (2.6%)	8.15×10^4 (2.6%)
≥7	4.48×10^4	2.51×10^4 (0.6%)	1.97×10^4 (0.6%)
Total	7.32×10^6	4.18×10^6 (100%)	3.14×10^6 (100%)

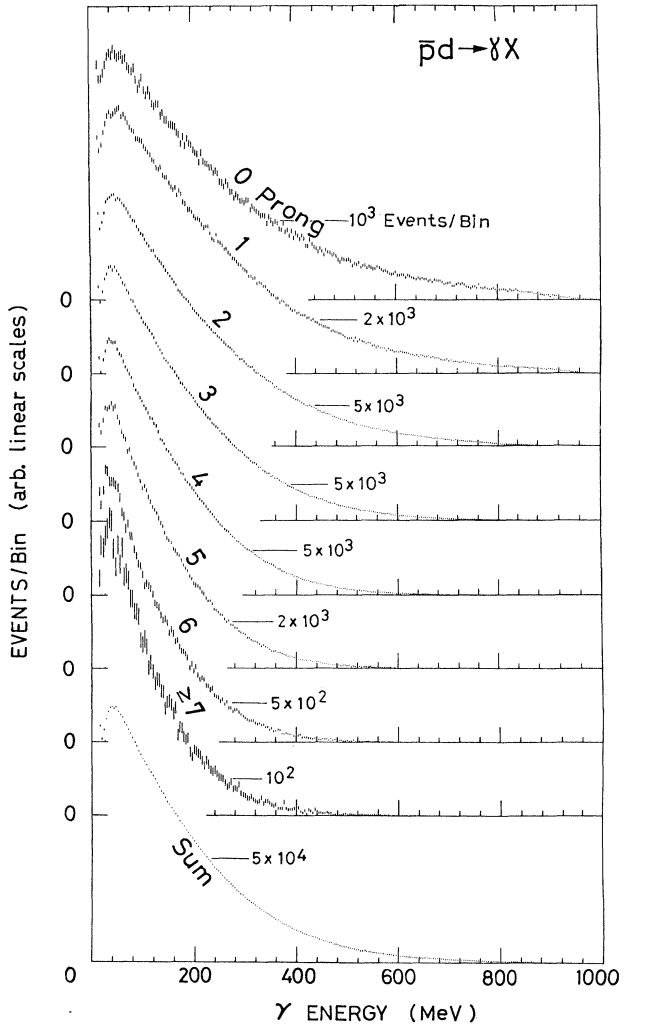

FIG. 1. Inclusive γ-ray spectra from $\bar{p}d$ annihilation at rest for each charge multiplicity as well as for their sum. Bars on the data points give the statistical error (1σ). Number of events per 4.16-MeV bin is given at an appropriate position on each spectrum to show the vertical scale.

where $q_{\bar{p}N}$ is the momentum of the annihilating $\bar{p}N$ in the laboratory system, q_F is the Fermi momentum (see the Appendix) of the nucleon in deuterium, and M_N is the nucleon rest mass. The first term comes from the purely instrumental width [1], the second one from the Doppler smearing due to the Fermi motion, and the last one from the shift of the γ energy due to the change in the $\bar{p}N$ rest mass. The estimation of the second term is given in the Appendix. The third term can be derived as follows: when we designate the nucleon momentum due to Fermi motion as q, the spectator nucleon and the $\bar{p}N$ system carry away kinetic energies of approximately $q^2/2M_N$ and $q^2/4M_N$, respectively. As a result, the $\bar{p}N$ rest mass scatters by

$$\Delta(M(\bar{p}N)) \sim 3q^2/4M_N \tag{7}$$

event by event. Then the ambiguity of the γ energy is approximately equal to $\Delta(M(\bar{p}N))$, when the γ energy is much smaller than M_N, and decreases with the increasing γ energy. We assume that the elementary process of baryonium production in $\bar{p}N$ annihilation should not prefer any specific values of q as far as q is small. Then the distribution of q which is effective in baryonium production can be simply calculated from the deuterium wave function. A numerical calculation with the Hulthen wave function for deuterium shows that about 75% of nucleons should have $q \leq q_F$ ($=104$ MeV/c, see the Appendix). Since the FWHM of Gaussian distribution corresponds to 75% lying within it, we may take $q \leq q_F$ to estimate the effect on the FWHM resolution $\Delta E/E$. The above consideration leads to the third term of Eq. (6). We actually neglected this term because it is much smaller than the first term as far as E is as large as 100 MeV or larger.

The modified instrumental resolution of Eq. (6) is plotted in Fig. 2. The FWHM resolution of 12% at 100 MeV and 7.9% at 900 MeV should be compared with 11% at 100 MeV and 6.4% at 900 MeV, respectively, obtained without the Doppler smearing.

Above 600 MeV, we have observed several peaks [21] which can be assigned to the two-meson annihilation of $\bar{p}p$ or $\bar{p}n \to \pi^0 M$ with π^0 mistaken as a single γ ray. Misidentification of $\pi^0 \to \gamma\gamma$ as a single γ ray was possible at high energies because of limited spatial resolution [2]. Except for the two-meson annihilation peaks and the so-called Panofsky γ-ray peak at 129 MeV, no narrow peak was seen between 80 and 938 MeV with statistical significance above 4σ. Only five narrow peaks at 2 to 3σ levels were obtained with the parameters given in Table II. The fit between 200 and 600 MeV is, after subtraction of the polynomial background, presented in Fig. 3 for the sum over the charge multiplicity, and in Fig. 4 for each charge multiplicity, separately.

The baryonium mass, calculated for the initial $\bar{p}N$ with the rest mass of $2M_N$, is also given in Table II. Since the $\bar{p}N$ rest mass in $\bar{p}d$ annihilation at rest is by $\Delta M_B = B + 3q^2/4M_N$ (here, $B \sim 2.23$ MeV, the binding energy of deuterium) below the threshold ($2M_N$), the correct baryonium mass should be less than the value given in the table by ΔM_B at the maximum (the case with the γ energy much less than M_N). Although the shift of ΔM_B scatters event by event, the center of the distribution corresponds to q with the largest phase-space density. Referring to the Appendix, this condition reads $q^2|\Psi(\mathbf{q})|^2 =$ maximum and occurs at $q \sim 43$ MeV/c for the Hulthen wave function. Substituting this value of q into ΔM_B, we obtain $\Delta M_B = 2.23 + 1.41 = 3.64$ MeV. Since this value is as small as or smaller than the ambiguity of baryonium mass due to the fitting error, we neglect it below.

C. Yields of peaks

The yield of $\bar{p}d \to \gamma B N_s$ with N_s a spectator proton or neutron or of $\bar{p}d \to \gamma B$ with B an $\bar{N}NN$ bound state was calculated in a similar way as for $\bar{p}p \to \gamma B$ [1]. The yield Y per $\bar{p}d$ annihilation is given by the number of monochromatic γ rays, i.e., the peak area A above the background, divided by the number of annihilations $N_{\bar{p}}$ corrected for the detection efficiency $\eta_B(E)$ of γ rays with the energy E as

$$\xi N_{\bar{p}} Y \eta_B(E) = A \ . \tag{8}$$

Here ξ is equal to α ($=0.571$), $1-\alpha$, and 1 when B can be produced only in $\bar{p}p$, only in $\bar{p}n$, and both in $\bar{p}p$ and $\bar{p}n$ annihilations, respectively. The last case of ξ is possible because the charge state of B was not measured very precisely. ξ is also unity for $\bar{p}d \to \gamma B$ with B an $\bar{N}NN$ bound state.

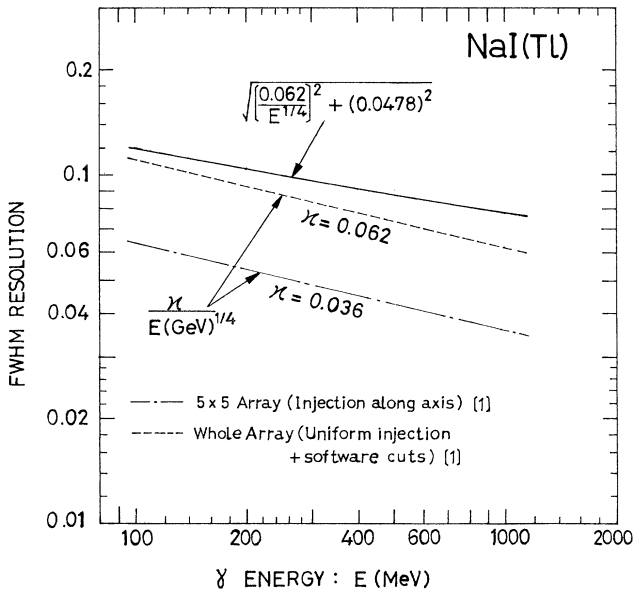

FIG. 2. The solid curve gives the modified energy resolution of the NaI calorimeter given by Eq. (6). Uniform injection of γ rays on NaI and application of software cuts including the cluster logics are assumed. The resolution without the Doppler smearing, etc. (dotted curve), and that of a 5×5 array of NaI modules for γ-ray injection along the central axis of the array (dash-dotted curve) are also shown for comparison.

TABLE II. Fitting result on narrow states seen in the inclusive γ-ray spectra. Position, yield per annihilation, statistical significance, and width are given for each peak. The width was made variable within the modified instrumental width [see Eq. (6)] +0%, −30%: (U) and (L) denote the upper and lower limits, respectively. For the case of U (or L), the error of width is meaningful only with the minus (or plus) sign, and is given in parentheses. The column of notes gives the weight-averaged position of the γ-ray peak. The mass of B for the assumed reaction of $\bar{p}N \rightarrow \gamma B$ is also given in parentheses (see the text).

	Charge multiplicity (N_{ch})									
	$N_{ch}=all$	0	1	2	3	4	5	6	≥7	Notes
Position (MeV)	124.5±2.4				121.2±2.8	126.0±1.9	132.2±3.9			125.0±1.3
Yield (10^{-3})	2.3±0.7				0.95±0.39	1.23±0.34	0.47±0.22			
Statistical significance	3.4σ				2.4σ	3.7σ	2.1σ			
Width σ (MeV)	8.5 (fix)				8.5 (fix)	8.5 (fix)	8.5 (fix)			
Position (MeV)			180.8±2.5				175.3±3.9		162.2±3.4	174.5±1.8
Yield (10^{-3})			0.35±0.14				0.26±0.12		0.06±0.03	$M_B=1693\pm2$
Statistical significance			2.5σ				2.1σ		2.1σ	
Width σ (MeV)			5.6 (2.0,L)				5.5 (2.3,L)		5.6±1.8	
Position (MeV)						328.2±5.3				328.2±5.3
Yield (10^{-3})						0.36±0.16				$M_B=1512\pm7$
Statistical significance						2.2σ				
Width σ (MeV)						9.1 (3.7,L)				
Position (MeV)	354.1±8.5		350.4±5.2	358.8±7.2		361.7±6.0				355.8±3.2
Yield (10^{-3})	0.98±0.48		0.33±0.12	0.43±0.20		0.28±0.14				$M_B=1479\pm5$
Statistical significance	2.1σ		2.6σ	2.1σ		2.1σ				
Width σ (MeV)	14.5±5.2		9.6 (4.0,L)	9.7 (2.8,L)		9.8 (3.6,L)				
Position (MeV)	472.4±6.8			470.1±8.4		480.3±5.5	454.4±6.5			470.2±3.3
Yield (10^{-3})	1.03±0.40			0.50±0.23		0.14±0.07	0.09±0.04			$M_B=1325\pm5$
Statistical significance	2.5σ			2.2σ		2.0σ	2.1σ			
Width σ (MeV)	17.8 (5.5,U)			17.7 (5.0,U)		12.4 (4.7,L)	11.8 (3.6,L)			
Position (MeV)	571.3±6.2	582.8±6.1	557.1±8.8							576.1±4.0
Yield (10^{-3})	0.69±0.31	0.17±0.08	0.21±0.10							$M_B=1167\pm7$
Statistical significance	2.3σ	2.0σ	2.1σ							
Width σ (MeV)	17.8±3.3	14.5 (5.5,L)	13.9 (5.9,L)							

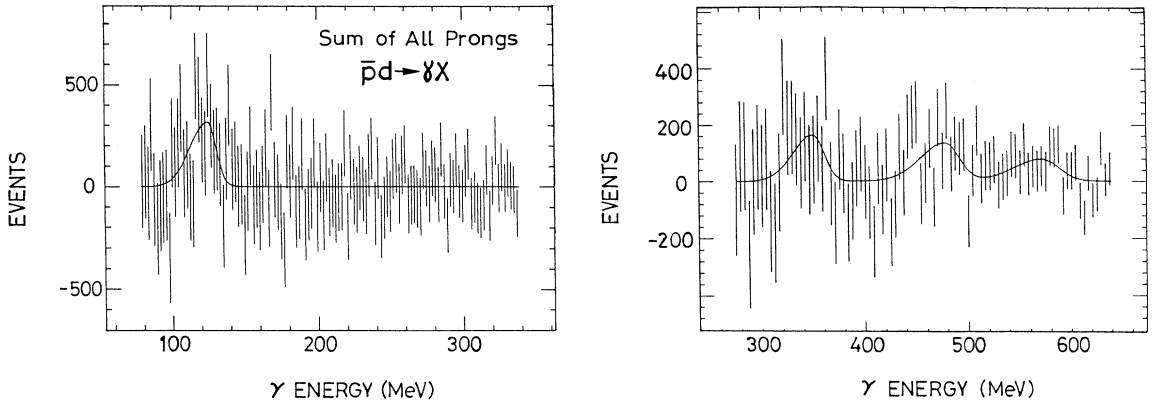

FIG. 3. The fitted result of the inclusive γ-ray spectra (see Fig. 1) below 600 MeV is shown for the sum over the charge-multiplicity after subtraction of the polynomial background.

Generally speaking, $\eta_B(E)$ should depend on the decay scheme of B as well as on the spectator nucleon. First we consider a quasifree process of $\bar{p}d \rightarrow \gamma B N_s$. Since the Fermi momentum in deuterium is as small as 104 MeV/c (see the Appendix), the spectator proton should mostly stop inside the target. Although the spectator neutron may come out, the kinetic energy is much less than the threshold (10 MeV) for γ-ray (or neutrals) detection. So, the detection efficiency of γ rays should hardly be affected. Approximately, therefore, $\eta_B(E)$ should not de-

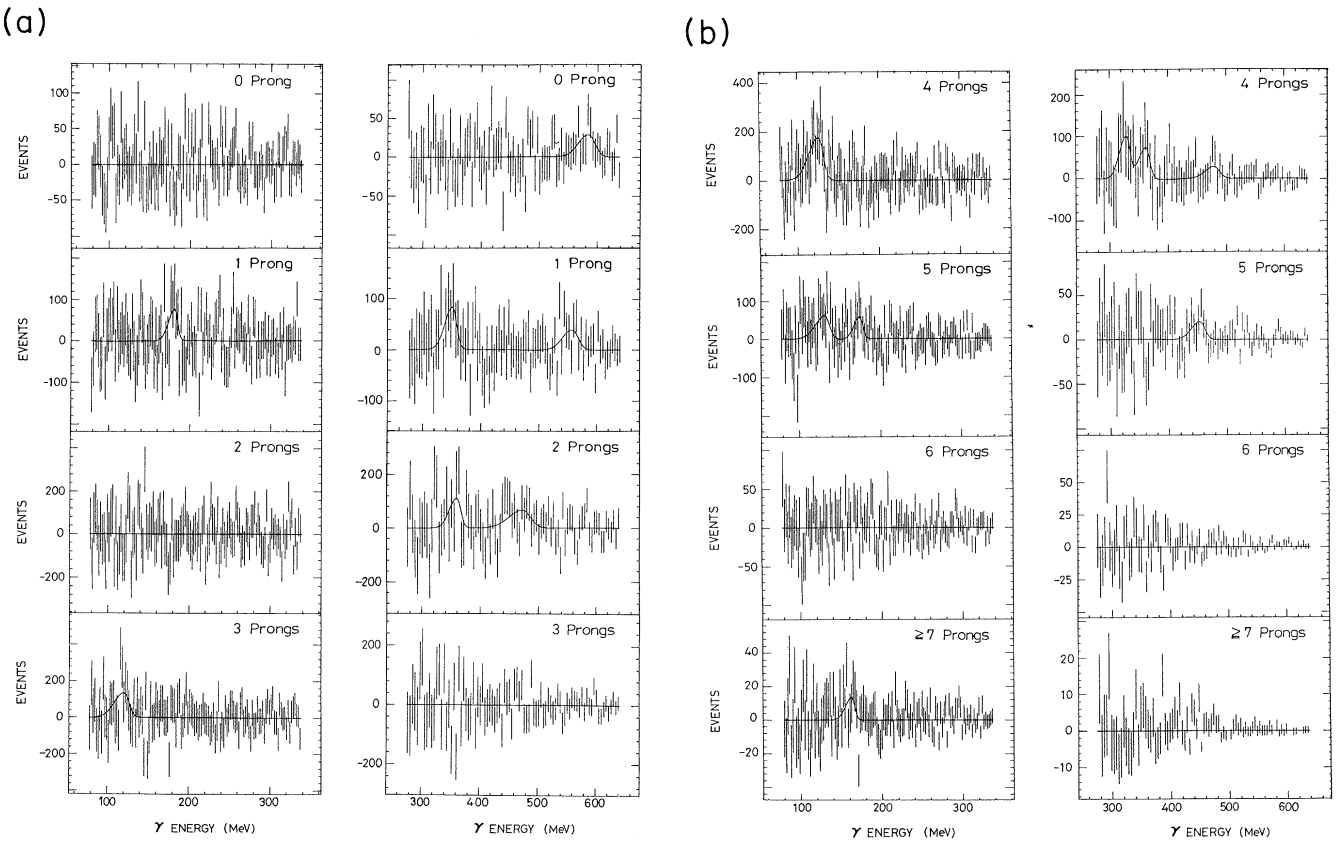

FIG. 4. The fitted result of the inclusive γ-ray spectra (see Fig. 1) below 600 MeV is shown for each charge multiplicity after subtraction of the polynomial background.

pend on the spectator nucleon. Since we do not know the decay scheme of B, we assume that its decay branching ratios into various channels are the same as in $\bar{p}p$ annihilation at rest. Then $\eta_B(E)$ can be taken the same as in $\bar{p}p$ annihilation at rest discussed in [1].

The situation is a little different for $\bar{p}d \to \gamma B$ with $B = \bar{N}NN$. In the decay

$$B \to (\text{mesons from } \bar{N}N) + N \ , \tag{9}$$

the nucleon may have enough energy to come out of the target, leading to a decrease in η_B. The decrease amounts to 0.015 in η_B per charged track or per γ ray (or a neutral which mimics a γ ray) as typically seen in Fig. 23 of [1], corresponding to about 10% of η_B. Since we do not know about the decay of the $\bar{N}N$ system in Eq. (9), we again assume that the decay branching ratios into various channels should be the same as in $\bar{p}p$ annihilation. Then $\eta_B(E)$ for $\bar{p}d \to \gamma B$ with $B = \bar{N}NN$ can be taken the same as the $\eta_B(E)$ for $\bar{p}p$ annihilation at rest [1] within an ambiguity of 10%. From the above consideration, we approximate $\eta_B(E)$ in Eq. (8) to be equal to the $\eta_B(E)$ in $\bar{p}p$ annihilation at rest given in [1].

As $N_{\bar{p}}$ in Eq. (8) is proportional to the number of γ-rays in the inclusive γ-ray spectrum (6.70×10^6), we obtain, by taking $\bar{p}d$ annihilation as the sum of quasifree $\bar{p}p$ and $\bar{p}n$ annihilations, another relation:

$$N_{\bar{p}} \int [\alpha \rho_p(E')\eta_p(E') + (1-\alpha)\rho_n(E')\eta_n(E')]dE' = N_\gamma \ . \tag{10}$$

Here $\rho_N(E')dE'$ with $N = p$, n is the number of γ rays (mostly coming from π^0) with the energy between E' and $E'+dE'$ per $\bar{p}N$ annihilation, and η_N is the detection efficiency of γ rays produced in $\bar{p}N$ annihilation.

According to the statistical models, for example, one by Orfanidis and Rittenberg [22], the charge multiplicity (mainly $\pi^{\pm}$) as well as the γ multiplicity (nearly twice the π^0 multiplicity) should be almost independent of $\bar{p}p$ or $\bar{p}n$ annihilation. This prediction is consistent with the experimental data listed in Table III. Then we may have an approximation of

$$\rho_p(E) = \rho_n(E) = \rho(E) \ , \tag{11}$$

where $\rho(E)$ is the number density of γ rays per $\bar{p}p$ annihilation discussed in [1]. Since η_N can be calculated once the charge and γ multiplicities in the final state are given, the above relation leads to an approximate equality of

$$\eta_p(E) = \eta_n(E) = \eta(E) \ , \tag{12}$$

where $\eta(E)$ is the detection efficiency of γ rays in $\bar{p}p$ annihilation at rest given in [1].

Substituting Eqs. (10)–(12) into Eq. (8), we obtain a simple equation:

$$Y = K(E)A/(\xi N_\gamma) \tag{13}$$

with

$$K(E) = \int \rho(E')\eta(E')dE'/\eta_B(E) \ ,$$

which is of the same form as in $\bar{p}p$ annihilation [1] except for the presence of ξ. $K(E)$ is the effective multiplicity of γ rays per $\bar{p}d$ (or $\bar{p}p$ or $\bar{p}n$) annihilation and is taken to be

$$K = 4.45 \tag{14}$$

within a systematic ambiguity of $\pm 20\%$ [1].

We have calculated the yield according to Eq. (13) with K given by Eq. (14). The obtained yields are given in Table II for the peaks with statistical significance higher than 2σ.

The most prominent peak comes from the Panofsky γ rays at 129 MeV. Its yield of 2.3×10^{-3} per $\bar{p}d$ annihilation is roughly consistent with an estimation (4.2×10^{-3}) which is derived by multiplying the following three numbers: the π multiplicity of 1.78 per $\bar{p}d$ annihilation [from α of Eq. (5) and the π^- multiplicity of 1.57 per $\bar{p}p$ and of 2.07 per $\bar{p}n$ annihilation as seen in Table III], the branching ratio $B(\pi^- d \to \gamma nn) = 0.25$ [26,27], and the average probability that a π^- meson should stop in the liquid $D_2 = 0.94\%$ corresponding to the pion range of 7 cm in deuterium. The last number was deduced from the π^- momentum distribution calculated by a Monte Carlo simulation [1] for $\bar{p}p$ annihilation. Since the π^- momentum distribution should depend on the model of $\bar{p}d$ annihilation mechanism, the last number may suffer from some ambiguity.

Except for the Panofsky γ-ray peak, we have seen five narrow peaks at photon energies of $E \sim 175$, 328, 356,

TABLE III. Charge-multiplicity $M_+ + M_-$, and γ multiplicity M_γ in $\bar{p}p$, $\bar{p}n$, and $\bar{p}d$ annihilation at rest.

	$M_+ + M_-$	M_γ	Reference
$\bar{p}p$	3.21±0.12	3.46±0.38	N. Horwitz *et al.* (1959) [23]
	2.99±0.08		T. Kalogeropoulos *et al.* (1980) [19]
	3.22	3.93	G. Backenstoss *et al.* (1983) [24]
$\bar{p}n$	3.15		V. Barnes (1964) [16]
	3.15		A. Bettini *et al.* (1967) [18]
	3.15±0.11		T. Kalogeropoulos *et al.* (1980) [19]
$\bar{p}d$	3.23±0.18	3.6±0.5	N. Horwitz *et al.* (1959) [23]
	3.04	3.77±0.08	T. Kalogeropoulos *et al.* (1974) [25]
	3.06±0.09		T. Kalogeropoulos *et al.* (1980) [19]

470, and 576 MeV with statistical significance of 2 to 3σ levels. The yields of these peaks are plotted in Fig. 5. The solid curves give the 4σ upper limit; it corresponds to four times the rms statistical fluctuation of the background γ rays, which are registered in an energy span of $\pm$ [modified instrumental FWHM given by Eq. (6)]. Although a few more peaks have been observed above 600 MeV in the γ-ray spectra, they are not shown in Fig. 5 since, as already described in the last paragraph of Sec. III B, all of them could be assigned to monochromatic π^0 peaks coming from $\bar{p}p$ or $\bar{p}n$ annihilation into $\pi^0 M$ with M one of known mesons.

In the low-energy region below 180 MeV, precision fitting was carried out by using an experimental Panofsky-peak spectrum instead of a Gaussian shape. We did this before in the analysis of γ-ray spectra from $\bar{p}p$ annihilation [1] because the Panofsky γ-ray spectrum, i.e., the spectrum of γ rays coming from annihilation of low-energy secondary π^- on proton, has a complicated structure consisting of a monochromatic peak at 129 MeV plus a broad peak between 55 and 83 MeV.

In $\bar{p}d$ annihilation, the γ rays arising from capture of secondary π^- by another deuterium should be localized dominantly around 129 MeV [26–28] corresponding to radiative capture of π^- ($\pi^- d \rightarrow \gamma nn$) with a far smaller amount of charge exchange ($\pi^- d \rightarrow \pi^0 nn \rightarrow \gamma\gamma nn$) which will produce a nearly box-type spectrum between 62 and 74 MeV. Consequently, the γ-ray spectrum from π^- capture should be much simpler in deuterium than in hydrogen. Actually, however, contamination of neutrons could make the apparent "γ-ray" spectrum complicated. Neutrons arising from $\pi^- d$ at rest into nn ($B \sim 75\%$ [26,27]) and γnn ($B \sim 25\%$ [26,27]) were mistaken as γ rays on NaI because no separation between γ rays and neutrons was made. The former could mimic γ rays with energies less than 68 MeV and the latter as small as 9 MeV.

Figure 6 shows the "γ-ray" spectrum from $\pi^- d$ annihilation at rest obtained in the present setup and with essentially the same data reduction procedure as for $\bar{p}d$ annihilation. The beam was changed from 580-MeV/c antiprotons to 167 MeV/c π^- so that π^- should stop around the target center. The γ-ray spectrum has a sharp peak around 129 MeV and an additional peak around 25 MeV with a broad tail toward higher energies. The latter structure may come from neutrons produced in $\pi^- d \rightarrow \gamma nn$ and $\pi^- d \rightarrow nn$. Although the kinetic energy of neutrons should be smaller than 68 MeV (in $\pi^- d \rightarrow nn$) for stopping π^-, neutrons from in-flight reactions should have higher energies. A small structure between 50 and 80 MeV may be interpreted in terms of the

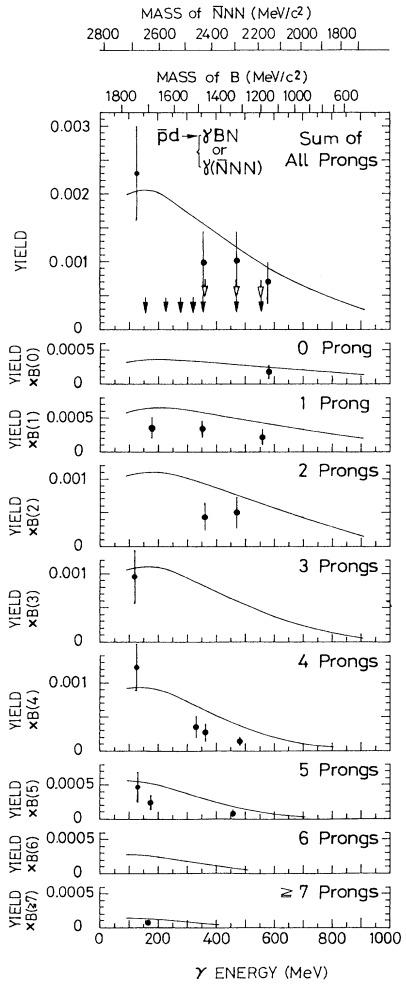

FIG. 5. The 4σ upper limit for the yield of narrow peaks (baryonia or $\bar{N}N$ bound states) is plotted with solid curves. Solid points show narrow peaks seen at 2 to 3σ levels. Solid and open arrows give the positions (except for the Panofsky peak at 129 MeV) where 2 to 3σ signals were observed in $\bar{p}p$ annihilation at rest into γX and $\pi^0 X$, respectively [1,2], with yields larger than 2×10^{-4} per annihilation.

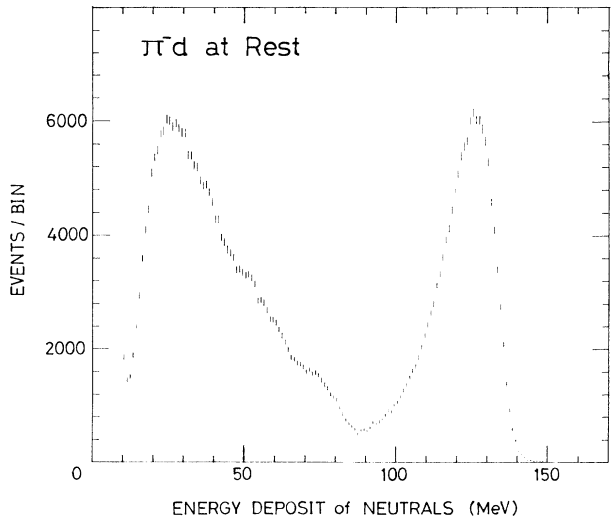

FIG. 6. An energy-deposit spectrum of γ rays and neutrons in the NaI detector for π^- capture in deuterium.

box-shape γ-ray spectrum between 55 and 83 MeV from π^- capture by contaminating hydrogen atoms, i.e., $\pi^- p \to \pi^0 n$ with $\pi^0 \to \gamma\gamma$. The amount of γ rays between 55 and 83 MeV above the smooth background curve was about 4% of the γ rays in the 129-MeV peak. Using the Panofsky ratio

$$P = B(\pi^- p \to \pi^0 n)/B(\pi^- p \to \gamma n) = 1.546 \pm 0.009$$

[29] and the branching ratio $B(\pi^- d \to \gamma nn) = 0.25$ [26,27], we find that the observed amount can be interpreted by contamination of H_2 in liquid D_2 by 0.9% (in mol). The above-mentioned structure may also include a small amount of photons coming from $\pi^- d \to \pi^0 nn$ with $\pi^0 \to \gamma\gamma$.

We have reanalyzed the γ-ray spectra from $\bar{p}d$ annihilation in the low-energy region of 30–180 MeV, using a high-statistics "γ-ray" spectrum from π^- capture by deuterium instead of a simple Gaussian. Each γ-ray spectrum was fitted with the sum of a polynomial background of order 3–4, the experimental γ-ray spectrum from π capture by deuterium, and any additional narrow Gaussians. The fitted result is presented in Figs. 7 and 8 after subtraction of the background. We have not observed any other new narrow peaks.

IV. SUMMARY AND DISCUSSION

We have carried out a high-statistics measurement of inclusive γ-ray spectra in $\bar{p}d$ annihilation at rest. Fitting the spectra with a polynomial background plus narrow Gaussian peaks, we have not observed any monochromatic γ-ray peaks which may be assigned to baryonium production $\bar{p}N \to \gamma B$ ($N = p$ or n) or $\bar{N}NN$ bound-state production $\bar{p}d \to \gamma(\bar{N}NN)$ at statistical significance above 4σ. The 4σ upper limit for the baryonium production per annihilation is plotted in Fig. 5; it varies between

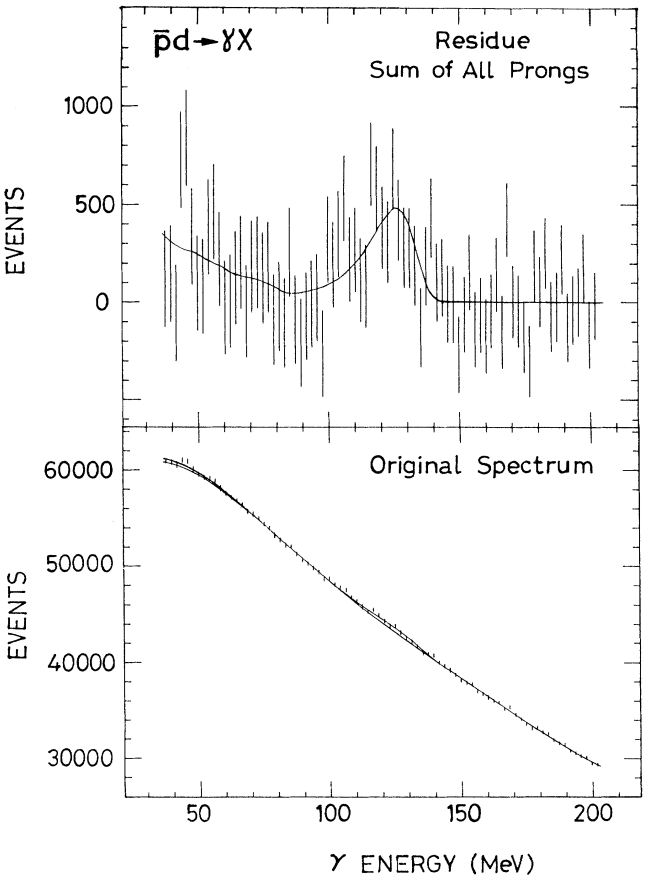

FIG. 7. A fit to the inclusive γ-ray spectrum summed over the charge multiplicity in the energy range of 40–200 MeV: original spectrum on the bottom and the residue after subtraction of the polynomial background on the top. An experimental spectrum for $\pi^- d \to \gamma nn$, $\pi^0 nn$ was used in fitting (see the text).

TABLE IV. Comparison of five γ peaks observed in the present experiment at 2-3σ levels with the corresponding γ or π^0 peaks observed before in $\bar{p}p$ annihilation at rest. The peak position gives the γ or π^0 energy at the peak. The mass of B in the reaction $\bar{p}d \to \gamma B N_s$ was deduced from the γ energy by assuming $\bar{p}N \to \gamma B$ with the initial $\bar{p}N$ at the threshold $2M_N$. Since the initial $\bar{p}N$ is actually below the threshold, the correct mass of B should be less than the value given in the table by 3.6 MeV at the maximum (see the text).

Reaction assumed	$\bar{p}d \to \gamma B N_s$ present expt.	$\bar{p}p \to \gamma B$ [1]	$\bar{p}p \to \pi^0 B$ [2]
Peak position (MeV)	174.5±1.8	156.4±2.4	
(mass of B in MeV)	(M_B = 1693±2)	(M_B = 1713±3)	
Peak position (MeV)	328.2±5.3	319.6±2.9	
(mass of B in MeV)	(M_B = 1512±7)	(M_B = 1524±4)	
Peak position (MeV)	355.8±2.3	355.9±7.0	362.2±2.3
(mass of B in MeV)	(M_B = 1479±5)	(M_B = 1478±9)	(M_B = 1483±5)
Peak position (MeV)	470.2±3.3	467.5±5.4	465.9±8.0
(mass of B in MeV)	(M_B = 1325±5)	(M_B = 1329±8)	(M_B = 1338±11)
Peak position (MeV)	576.1±4.0	560.3±6.3	562.2±3.1
(mass of B in MeV)	(M_B = 1167±7)	(M_B = 1191±10)	(M_B = 1197±6)

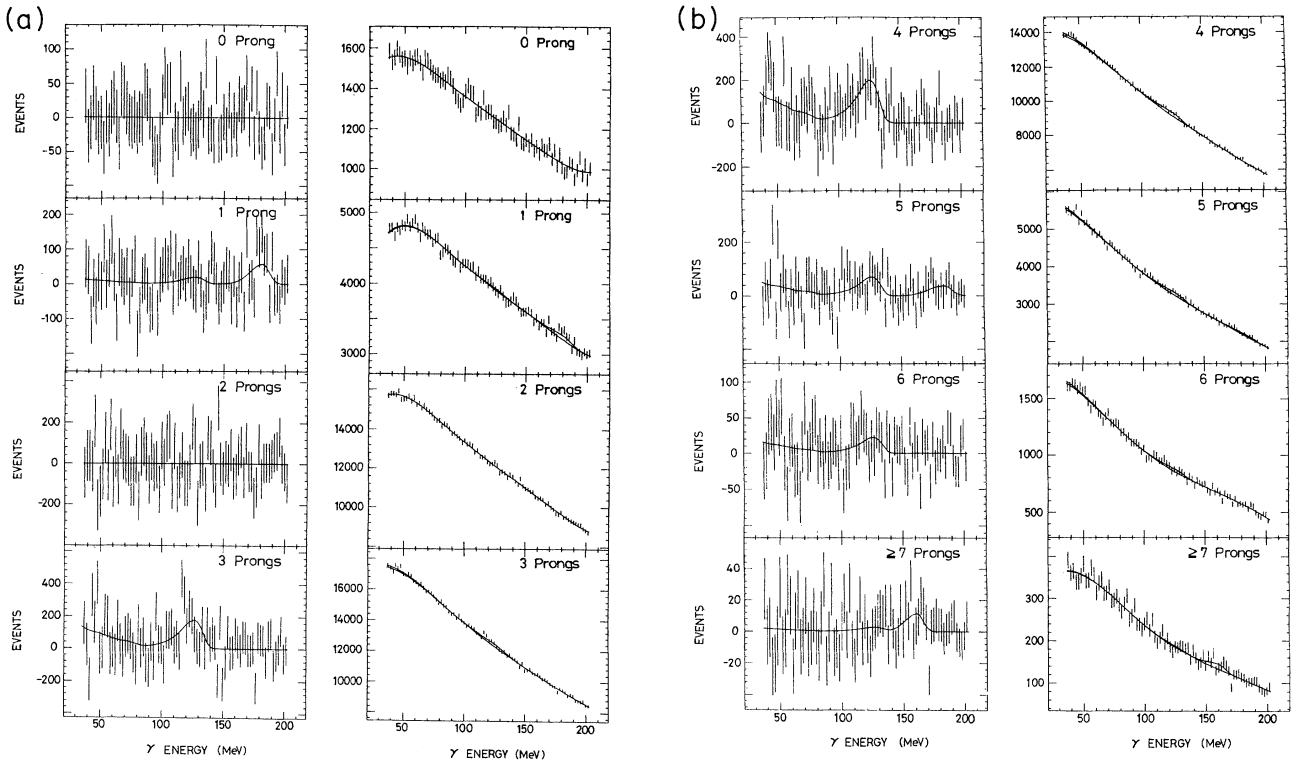

FIG. 8. A fit to the inclusive γ-ray spectrum in the energy range 40–200 MeV for each charge multiplicity separately. Original spectra are shown on the right-hand side and the residue on the left-hand side. The other items are the same as in Fig. 7.

10^{-2} and 10^{-4} depending on the baryonium mass and the charge multiplicity.

The above result indicates, within the sensitivity given in Fig. 5 and above the γ energy of 40 MeV, the following: (i) absence of narrow baryonia produced in $\bar{p}n \rightarrow \gamma B$, (ii) absence of baryonia in $\bar{p}p \rightarrow \gamma B$ even for $\bar{p}p$ in the orbital P state, and (iii) absence of $(\bar{N}NN)$ bound states in $\bar{p}d \rightarrow \gamma$ $(\bar{N}NN)$.

Five narrow peaks were observed at 2 to 3σ levels at photon energies of 175 MeV (the corresponding B mass, $M_B = 1693$ MeV/c^2 when $\bar{p}d \rightarrow \gamma B N_s$ is assumed), 328 MeV ($M_B = 1512$ MeV/c^2), 356 MeV ($M_B = 1479$ MeV/c^2), 470 MeV ($M_B = 1325$ MeV/c^2), and 576 MeV ($M_B = 1167$ MeV/c^2). Three of the above five peaks, except for the 175- and 328-MeV ones, are located close to the 2-3σ peaks which we have observed in $\bar{p}p$ annihilation at rest to γX [1] (the position given in Fig. 5 with solid arrows) and in $\bar{p}p$ annihilation at rest to $\pi^0 X$ [2] (open arrows). Although the coincidence of the peak positions between the $\bar{p}p$ and $\bar{p}d$ annihilations seems remarkable (see Table IV), it is difficult to draw a definite conclusion at the present stage, since the significance of the peaks observed is not large. A search for narrow γ lines with an order-of-magnitude higher statistics could give a definite conclusion.

ACKNOWLEDGMENTS

The authors express their deep thanks to Professor T. Nishikawa, Professor S. Ozaki, Professor H. Sugawara, Professor H. Hirabayashi, and Professor K. Nakai for supporting the present work, and to the staff of the computer center of KEK for giving valuable help during the analysis.

APPENDIX: DOPPLER SMEARING OF γ ENERGIES

1. Momentum of annihilating $\bar{p}N$ system in the laboratory system

Antiproton annihilation in deuterium occurs from $\bar{p}N$ ($N = p$ or n) moving in the laboratory system. One of the contributions to the momentum of the $\bar{p}N$ system comes from the momentum $\mathbf{q}$ of the Fermi motion of each nucleon in deuterium. Another contribution comes from the kinetic energy of antiprotons acquired from the potential energy when the antiproton annihilates at the nuclear surface. The corresponding momentum of the antiproton is given by $\mathbf{q}_{\bar{p}}$ in Eq. (2). The deuterium carries the opposite momentum. Because only one of the two nucleons of the deuterium interacts with $\bar{p}$, it carries $-\frac{1}{2}\mathbf{q}_{\bar{p}}$. As a result, the momentum of the $\bar{p}N$ system is $\frac{1}{2}\mathbf{q}_{\bar{p}}$ in the laboratory system. By summing the above two contributions, the total momentum of the annihilating $\bar{p}N$ system in the laboratory system is

$$\mathbf{q}_{\bar{p}N} = \mathbf{q} + \tfrac{1}{2}\mathbf{q}_{\bar{p}} \ . \tag{A1}$$

2. Estimation of the Fermi momentum q_F

The deuterium wave function is given, apart from a normalization factor, by

$$\Psi^M(\mathbf{r})=[u(r)/r]Y^M_{101}+[w(r)/r]Y^M_{121} , \quad \text{(A2)}$$

where $\mathbf{r}=\mathbf{r}_p-\mathbf{r}_n$ is the relative position vector of the two nucleons, and $u(r)$ and $w(r)$ are the radial wave functions of the S and D waves, respectively. Since the amount of the D wave is as small as 6–7 % [30], the relative momentum between proton and neutron may be determined almost completely by the S wave. The momentum ($\mathbf{q}$) distribution of the proton or neutron is given by $|\Psi(\mathbf{q})|^2 d\mathbf{q}$, where $\Psi(\mathbf{q})$ is the Fourier transform of $\Psi(\mathbf{r})$ and is reduced, apart from normalization, to

$$\Psi(\mathbf{q})=(1/2iq)\int (e^{iqr}-e^{-iqr})u(r)dr . \quad \text{(A3)}$$

When the Hulthen wave function [31]

$$u(r)=\exp(-\alpha r)-\exp(-\beta r) \quad \text{(A4)}$$

is used, we obtain

$$\Psi(\mathbf{q})=(q^2+\alpha^2)^{-1}-(q^2+\beta^2)^{-1} . \quad \text{(A5)}$$

Here,

$$\alpha=(MB)^{1/2}\hbar=(4.31\ \text{fm})^{-1}=45.8\ \text{MeV}/c \quad \text{(A6)}$$

for the deuterium binding energy $B=2.225$ MeV [31] and β is numerically estimated to be

$$\beta\cong 5.181\alpha \quad \text{(A7)}$$

[32] from nucleon-nucleon scattering data at low energies.

Since q_F is given by the rms value of q, we obtain

$$q_F=\left[\int q^2|\Psi(\mathbf{q})|^2 d\mathbf{q}\Big/\int|\Psi(\mathbf{q})|^2 d\mathbf{q}\right]^{1/2}$$
$$=(\alpha\beta)^{1/2}\sim 104\ \text{MeV}/c . \quad \text{(A8)}$$

3. Doppler smearing

The annihilating $\bar{p}N$ system is moving with respect to the laboratory system with a velocity of

$$\beta_G=q_{\bar{p}N}/(2M_N)\sim[q^2+(q_{\bar{p}}/2)^2]^{1/2}/(2M_N) . \quad \text{(A9)}$$

Since q is represented by q_F, which is much larger than $q_{\bar{p}}/2$ (~ 10.6 MeV/c) in deuterium, the approximate magnitude of β_G is $q_F/(2M_N)=0.055$.

The photon energy k in the laboratory system is different from the corresponding quantity k^* in the center-of-mass system of $\bar{p}N$, depending on the Fermi motion along the direction of the boost. We obtain a relation

$$k\sim k^*-\beta_G(\mathbf{k}^*\cdot\mathbf{q}_{\bar{p}N})/q_{\bar{p}N}=k^*-(\mathbf{k}^*\cdot\mathbf{q}_{\bar{p}N})/2M_N , \quad \text{(A10)}$$

neglecting the higher-order terms in β_G. Since the direction of $q_{\bar{p}N}$ is distributed uniform with respect to the photon vector, the rms value of $(\mathbf{k}^*\cdot\mathbf{q}_{\bar{p}N})$ is $k^*q_{\bar{p}N}/\sqrt{3}$. Then we obtain

$$\sigma(k)/k\sim\beta_G/\sqrt{3}=q_{\bar{p}N}/(2\sqrt{3}M_N) , \quad \text{(A11)}$$

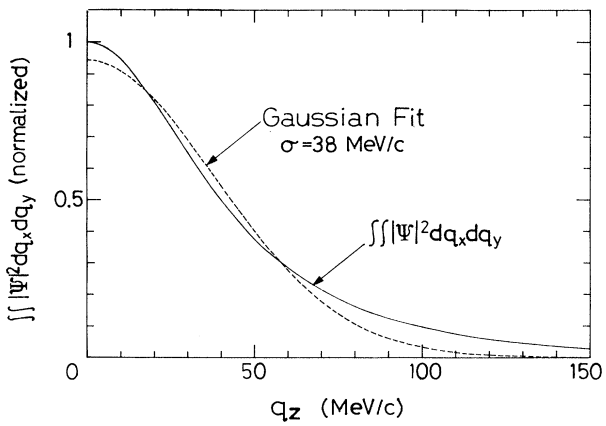

FIG. 9. $\int\int|\Psi(\mathbf{q})|^2 dq_x\, dq_y$, the two-dimensional integral of the Hulthen wave function squared for deuterium (see the text) is shown in comparison with the best fit by a Gaussian shape with $\sigma=38$ MeV/c.

which directly gives Eq. (6). Approximating q by q_F in $q_{\bar{p}N}$ of Eq. (A1) and neglecting $\frac{1}{2}q_{\bar{p}}$ compared with q_F, we get

$$\sigma(k)/k\sim q_{F\|}/(2M_N) , \quad \text{(A12)}$$

where $q_{F\|}=q_F/\sqrt{3}$ is the Fermi momentum along the photon vector.

4. Effect of Doppler smearing on the instrumental γ-energy resolution

In the search for narrow peaks in the inclusive γ-ray spectra, we used for simplicity the Gaussian shape for the peaks. In this approximation, Doppler smearing of the γ energy is also taken to be of a Gaussian shape. Since the smearing is related to the Fermi momentum along the photon vector according to Eq. (A12), we should use for $q_{F\|}$ its effective value $q_{F\|}(\text{eff})$, which can be obtained by approximating the Fermi momentum distribution along the photon vector by a Gaussian function as

$$\int\int|\Psi(\mathbf{q})|^2 d^2q_\perp\sim\text{const}\times\exp\{-[q_\|/q_{F\|}(\text{eff})]^2/2\} . \quad \text{(A13)}$$

For the Hulthen wave function of Eq. (A5), the left-hand term becomes, apart from a constant factor,

$$A^{-1}+B^{-1}+2\ln(A/B)/(B-A) \quad \text{(A14)}$$

with $A=\alpha^2+q^2$ and $B=\beta^2+q^2$. The best fit over the region of $k=0$–150 MeV/c is obtained with $q_{F\|}(\text{eff})=38$ MeV/c (see Fig. 9). This value does not vary by more than 1% even if the fitted region is extended up to 200 MeV/c. Substituting the above value of $q_{F\|}(\text{eff})$ into $q_{F\|}$ of Eq. (A12), we finally obtain

$$\sigma(k)/k\sim q_{F\|}(\text{eff})/(2M_N)\sim 0.0203 . \quad \text{(A15)}$$

Although the Gaussian approximation should cause an underestimate of the yield of narrow γ-ray peaks, its amount should be much less than 10% from the difference between the areas below the $\int\int|\Psi(\mathbf{q})|^2 d^2q_\perp$ curve and below its Gaussian fit.

*Present address: Kochi Medical School, Nankoku, Kochi, 783 Japan.
†Present address: KEK, National Laboratory for High Energy Physics, Tsukuba, 305 Japan.
‡Present address: Naruto University of Education, Naruto, Tokushima, 772 Japan.

[1] M. Chiba *et al.*, Phys. Lett. B **177**, 217 (1986); M. Chiba *et al.*, Phys. Rev. D **36**, 3321 (1987).
[2] M. Chiba *et al.*, Phys. Lett. B **202**, 447 (1988).
[3] A. Angelopoulos *et al.*, Phys. Lett. B **178**, 441 (1986).
[4] L. Adiels *et al.*, Phys. Lett. B **182**, 405 (1986).
[5] B. Richter *et al.*, Phys. Lett. **126B**, 284 (1983).
[6] L. Gray *et al.*, Phys. Rev. Lett. **26**, 1491 (1971).
[7] C. Amsler *et al.*, Phys. Rev. Lett. **44**, 853 (1980).
[8] D. Bridges *et al.*, Phys. Rev. Lett. **56**, 211 (1986); **56**, 215 (1986); **57**, 1534 (1987); I. Daftari *et al.*, Phys. Rev. Lett. **58**, 859 (1987).
[9] L. Adiels *et al.*, Phys. Lett. **138B**, 235 (1984).
[10] L. Adiels *et al.*, Z. Phys. C **35**, 15 (1987). M. Chiba *et al.*, Phys. Rev. D **38**, 2021 (1988).
[11] H. Poth *et al.*, Phys. Lett. **76B**, 523 (1978).
[12] L. Gray *et al.*, Phys. Rev. Lett. **30**, 1091 (1973).
[13] C. R. Sun *et al.*, Phys. Rev. D **14**, 1188 (1971).
[14] O. D. Dal'karov *et al.*, Yad. Fiz. **17**, 1321 (1973) [Sov. J. Nucl. Phys. **17**, 688 (1973)].
[15] T. E. Kalogeropoulos *et al.*, Phys. Rev. Lett. **35**, 824 (1975).
[16] V. Barnes, in *Pion and Kaon Production in Antiproton-Neutron Annihilation at Rest,* Proceedings of the 12th International Conference on High Energy Physics, Dubna, U.S.S.R., 1964, edited by Ya. A. Smorodinskii *et al.* (Aromizdat, Moscow, 1966), p. 764.
[17] W. Chinowsky *et al.*, Nuovo Cimento **43**, 684 (1966).
[18] A. Bettini *et al.*, Nuovo Cimento A **47**, 642 (1967).
[19] T. K. Kalogeropoulos *et al.*, Phys. Rev. D **22**, 2585 (1980).
[20] F. James and M. Roos, Comput. Phys. Commun. **10**, 343 (1975).
[21] The result on the observed γ-ray peaks above 600 MeV due to two-meson annihilation will be presented elsewhere together with the result on the inclusive π^0 spectra (under analysis) from $\bar{p}d$ annihilation at rest.
[22] S. J. Orfanidis and V. Rittenberg, Nucl. Phys. **B59**, 570 (1973).
[23] N. Horwitz *et al.*, Phys. Rev. **115**, 472 (1959).
[24] G. Backenstoss *et al.*, Nucl. Phys. **B228**, 424 (1983).
[25] T. E. Kalogeropoulos *et al.*, Phys. Rev. Lett. **33**, 1635 (1974).
[26] P. K. Kloeppel, Nuovo Cimento **34**, 11 (1964).
[27] J. W. Ryan, Phys. Rev. **130**, 1554 (1963).
[28] R. MacDonald *et al.*, Phys. Rev. Lett. **38**, 746 (1977).
[29] T. Spuller *et al.*, Phys. Lett. **67B**, 479 (1977).
[30] See, for example, M. A. Preston and R. K. Bhaduri, *Structure of Nucleus* (Addison-Wesley, Reading, MA, 1975).
[31] See, for example, M. L. Goldberger and K. M. Watson, *Collision Theory* (Wiley, New York, 1967).
[32] M. Moravcsik, Nucl. Phys. **7**, 113 (1958).